Colloid Polym Sci 277:868–874 (1999)

ORIGINAL CONTRIBUTION

V. Garamus
K. Kameyama
R. Kakehashi
H. Maeda

Neutron scattering and electrophoresis of dodecyldimethylamine oxide micelles

Received: 3 March 1999
Accepted in revised form: 22 April 1999

V. Garamus
Frank Laboratory of Neutron Physics
Joint Institute for Nuclear Research
141980 Dubna, Russia

V. Garamus
GKSS Research Center, D-21502
Geesthacht, Germany

K. Kameyama
Department of Biomolecular Science
Faculty of Engineering Gifu University
Gifu 501-1193, Japan

Rie Kakehashi[1] · H. Maeda (✉)
Department of Chemistry
Faculty of Science Kyushu University
Fukuoka 812-8581, Japan
e-mail: h.maescc@mbox.nc.kyushu-u.ac.jp
Fax: +81-92-6422607

[1] *Present address*: Osaka Municipal
Technical Research Institute, Morinomiya
Osaka 536-8553, Japan

Abstract Small-angle neutron scattering (SANS) measurements were carried out at 25 °C on dodecyldimethylamine oxide solutions under different conditions. In media with no added salt, the micelle aggregation number remained nearly constant (70–78) over the range of the degree of ionization, α_M, between 0 and 0.73 in contrast with the sharp critical micelle concentration increase in a narrow range of α_M from 0.35 to 0.40. This characteristic α_M dependence that deviates markedly from the prediction of the regular solution approach is thus shown to take place without a considerable change with respect to micelle size and shape. The surface electric potential employed to calculate the intermicellar repulsion under the Debye–Hückel approximation was found to be much lower than the actual surface potential determined from hydrogen ion titration. This inconsistency was solved by introducing a rescaled particle size for the hard-sphere interaction part. The surface potential from SANS was rather similar to the zeta potential determined by electrophoretic light scattering. In the range of NaCl concentrations higher than about 0.2 M, micelle growth was observed for both the hemihydrochloride (1:1 complex) and the cationic species and the growth into a cylindrical shape was confirmed.

Key words Small-angle neutron scattering · Electrophoretic light scattering · Dodecyldimethylamine oxide · Intermicelle interaction

Introduction

Dodecyldimethylamine oxide (DDAO) exists as either a nonionic or a cationic (protonated form) species depending on the pH of the aqueous solution and various solution properties vary with pH [1–16]. We have found that the aggregation number of DDAO exhibits a maximum around the half-ionized state when the degree of ionization of the micelle, α_M, is varied [11]. The interactions giving rise to this characteristic dependence were correlated with the characteristic pH dependences of the critical micelle concentrations (cmc), as shown by Rathman and Christian [7] and Maeda et al. [12]. General correlation of this kind has been discussed extensively by Hoffmann [17]. Surface excess at the air–water interface was a maximum in the range of α_M near 0.5 [12, 13]. In the hydrogen ion titrations the intrinsic dissociation constant of the amine oxide group on the micelle surface is known to be smaller than that of the monomer [3, 4]. These characteristic properties have been interpreted in terms of hydrogen-bond formation between the nonionic and the cationic pair [13]. Our later study [14] on the effects of ionic strength on the cmc of DDAO revealed an interesting result that the cmc of the cationic species is lower than that of the nonionic one at high ionic strengths (higher than 0.2 M NaCl). A hydrogen bond for the cationic–cationic pair is suggested.

Small-angle neutron scattering (SANS) has been successfully applied to elucidating the microstructure and the interparticle interaction of surfactant micelles and their liquid-crystalline phases [18–20]. In most of the previous SANS studies on amine oxides, the effect of protonation has been neglected [21, 22]. Tetradecyldimethylamine oxides form rodlike micelles even in the nonionic state [22]. In the present study, we have examined DDAO micelles by means of SANS and electrophoretic light scattering (ELS) with particular attention to the effect of protonation.

Experimental

DDAO used in this study was the same sample as used previously [12, 14]. The micelle compositions were very close to the overall one in the present study but they were examined on the basis of the apparent pH obtained with a glass electrode in D_2O solutions after due corrections.

SANS measurements were performed on the "MURN" time-of-flight, SANS spectrometer of the IBR-2 pulsed reactor at FLNP JINR, Dubna, Russia. The spectrum of the incoming thermal neutrons is characterized by the Maxwell distribution and an average wavelength of 1.1 Å. The samples were placed in quartz cells (Helma) with a 1-mm path; a 1-cm^2 area was illuminated by the neutron beam. The systematic errors of the neutron scattering cross section values did not exceed 5% [23]. Incoherent scattering backgrounds were subtracted using the measured equivalent of H_2O/D_2O solutions. The scattering vector range was from 0.008 to 0.4 $Å^{-1}$. The measurements were repeated twice (12 h between experiments) and no changes between scattering curves were observed. Throughout the data analysis, corrections were made for instrumental smearing [24].

ELS measurements were carried out with a Photal ELS-800 (Otsuka Electronics Co.) with a He–Ne laser as a light source on solutions with no added salt and the surfactant concentration was 30 mM. A rectangular quartz cell (internal dimensions: 2 mm in height, 10 mm in width and 17 mm in length) separated a pair of Pt/Pt black electrode chambers connected through semipermeable membranes. The temperature of the cell was maintained at 25 °C by circulation of thermostated water through the mounting block of the cell. Sample solutions were introduced into the cell by a peristaltic pump after being filtered with a Millipore membrane (pore size 0.2 μm). The electrophoretic mobility, u, was determined from the electro-osmotic plots of six or seven points in the cell for each sample. For each point 30–100 transients were accumulated to obtain correlation functions of good quality. The diffusion constants of the micelles were obtained from measurements of the homodyne mode.

Results

SANS of the solutions with no added salt

Neutron scattering curves of aqueous solution of DDAO in the absence of added salt at varying degrees of ionization are showed in Fig. 1. The scattering curve of the solution with zero degree of ionization (Fig. 1A) represents the scattering of an ensemble of noninteractive aggregates. The scattering from other solutions (Fig. 1B) exhibits an interference maximum suggesting a long-range interaction among aggregates in the system which can be connected with the electrical charge of the aggregates. The further analysis of the scattering results involves the modelling of the solution by an ensemble of particles (two-shell ellipsoid) with a screened Coulomb potential.

In the case of monodisperse spheres of number density n, the expression for the differential cross sections of neutron scattering per unit volume, $d\Sigma(q)/d\Omega$, versus the scattering vector $q = 4\pi\sin\theta/\lambda$ (2θ is the scattering angle and λ is the wavelength) can be written as follows [25]

$$d\Sigma(q)/d\Omega = nP^2(q)S(q) \quad , \qquad (1)$$

Fig. 1A, B Neutron scattering curves of dodecyldimethylamine oxide (*DDAO*) in solutions with no added salt at different micelle compositions. The micelle composition was given as the mole fraction of the cationic species or the degree of ionization, α_M. Surfactant concentration c_D = 20–21 mM. **A** Nonionic micelle ($\alpha_M = 0$). **B** Nonionic–cationic mixed micelles: $\alpha_M = 0.29(\square)$, $0.37(\Delta)$, $0.52(\nabla)$, $0.79(\bigcirc)$. The *solid curves* represent the fitting curves

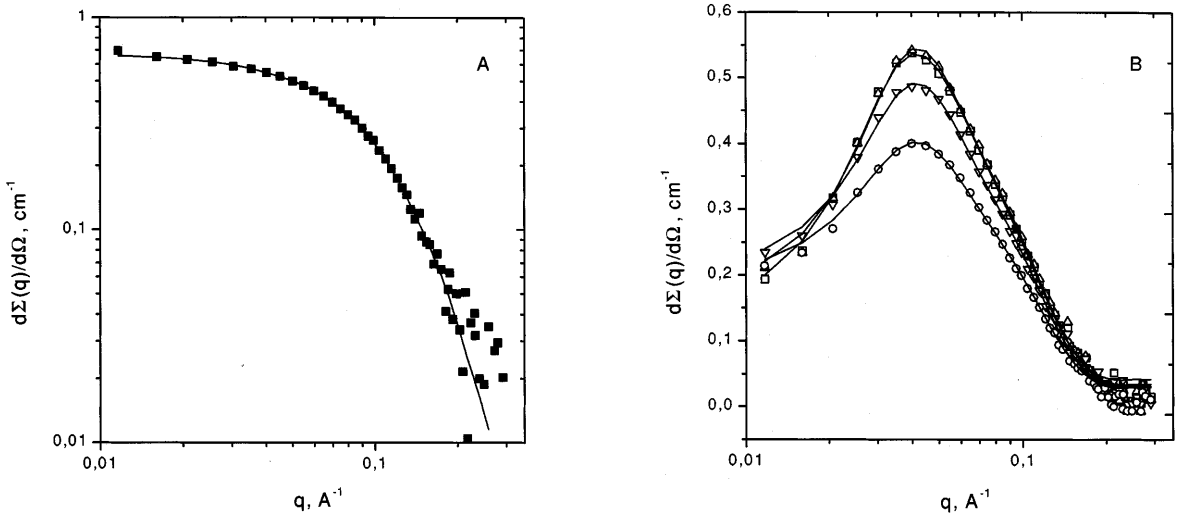

where the form factor $P^2(q)$, which expresses the scattering cross section of one particle, is

$$P^2(q) = \left[\int (\rho(r) - \rho_s)\exp(iqr)\,dv\right]^2 \quad , \tag{2}$$

where $\rho(r)$ is the scattering-length density of a particle with radius r, and ρ_s is the scattering-length density of the solvent. The structure factor $S(q)$ is defined by

$$S(q) = 1 + V^{-1}\int (g(r) - 1)\exp(iqr)\,dv \quad , \tag{3}$$

where $g(r)$ is the radial distribution function of the particles and V is the volume of the solution per particle.

In the case of polydisperse or nonspherical particles, $d\Sigma(q)/d\Omega$ can be written as

$$d\Sigma(q)/d\Omega = n[\langle|P(q)|\rangle^2 S(q) + (\langle|P(q)|^2\rangle - \langle|P(q)|\rangle^2)] \quad . \tag{4}$$

The decoupling approximation [26], that there is no correlation between interparticle separation and particle size and that there is no correlation between the separation of the particles and their orientation, could be used to calculate the second term of Eq. (4).

In the present study, the micelles are assumed to be monodisperse, prolate two-shell ellipsoids of volume V_2 with semiaxes a, b and b. The inner shell is the hydrocarbon core of volume V_1 with a scattering length density ρ_1; the outer shell is volume of $(V_2 - V_1)$ with scattering length density ρ_2. The definition of the single-particle scattering function is given by

$$P^2(q) = \int_0^{\pi/2} [(\rho_1 - \rho_2)V_1F(q,R_1) + (\rho_2 - \rho_s) \times (V_2 - V_1)F(q,R_2)]^2 \sin(\mu)\,d\mu \quad , \tag{5}$$

where $F(q,R_i) = 3[\sin(x) - x\cos(x)]/(x)^3$, $x = qR_i$, $R_i(\mu) = b_i[1 + \mu^2\{(a_i/b_i)^2 - 1\}]^{1/2}$ with μ denoting the cosine of the angle between the q vector and the long axis a.

The volumes and radii are calculated by assuming that each micelle consists of m (mean aggregation number) surfactant molecules. The hydrocarbon core volume V_1 was calculated according to Tanford [27]. The volume V_2 is defined as follows:

$$V_2 - V_1 = m\{\nu[NO(CH_3)_2H] + \varpi_{HG}\nu(D_2O) + \theta[\nu(Cl^-) + \varpi_{Cl}\nu(D_2O)]\} \quad . \tag{6}$$

In Eq. (6), $\nu[NO(CH_3)_2H]$, $\nu(Cl^-)$, and $\nu(D_2O)$ are the volumes of the head group, chloride ion and D_2O, respectively. The hydration number of the head groups of DDAO, ϖ_{HG}, was approximated as a constant irrespective of the micelle composition. ϖ_{Cl} stands for the hydration number of the chloride ion and θ is the degree of chloride counterion binding. The numerical values of the volumes and of the hydration numbers ($\varpi_{HG} = 5$ and $\varpi_{Cl} = 5$) were taken from Ref. [28].

The interaction potential between spherical macroions with a screened Coulomb potential is given as follows [29]:

$$V_c(r) = \pi\varepsilon\varepsilon_0\langle d\rangle^2\psi_0^2\exp[-\kappa(r - \langle d\rangle)]/r, \quad r > \langle d\rangle \tag{7}$$

where $\langle d\rangle$ is the rescaled diameter of the particle, r is the interionic centre-to-centre distance, ψ_0 is the effective surface potential, ε_0 is the permeability of free space and ε is the dielectric constant of the solvent medium. Here, κ is the usual Debye–Hückel inverse screening length, determined by the ionic strength of the solution. The monomers of the cationic species play the role of a salt in the present study. Under the assumption leading to Eq. (7), the surface potential is related to the effective charge ze_0 on the micelle by Eq. (8).

$$\psi_0 = ze_0/[\pi\varepsilon\varepsilon_0\langle d\rangle(2 + \kappa\langle d\rangle)] \quad . \tag{8}$$

We used the rescaled mean spherical approximation structure factor for dilute charged colloidal dispersions calculated by Hansen and Hayter [30]. For the fitting procedure, we used a FORTRAN program written by Hayter.

The fitting parameters were the aggregation number, the degree of counterion binding, θ, the residual background, the normalization parameter, and then micellar radius, charge and potential were calculated. The number of fitting parameters corresponds to the information content of the scattering patterns [31]. The model describes the experimental data satisfactorily (Figs. 1, 4). In our case, the fit resulted in a good approximation to the experimental points in the region of the scattering vector ($q < 0.3\,\text{Å}^{-1}$), which corresponds to the spacing and mean size of the micelles. We used the values of the mean aggregation number and the electrical charge of the micelles. The value of the axial ratio did not exceed 2.5, and the residual background was less than $0.01\,cm^{-1}$. The values of the fitting parameters are presented in Table 1.

In Fig. 2 the mean aggregation numbers obtained from the SANS study scarcely depend on the micelle composition in contrast with the marked dependence in media of moderate ionic strength (a maximum near 1:1 composition) [11]. The cmc values in the solutions without added salt, taken from Ref. [15], are also shown in Fig. 2. The observed composition dependence of the cmc differs markedly from the prediction of the regular solution approximation [32, 33] as shown in Fig. 3. It is not surprising that the regular solution approach does not work in the case of the ionic micelles in media of low ionic strength as encountered in the present study. Nevertheless, various ionic/nonionic mixed micelles in solutions with no added salt have been reported to be well-described by the regular solution approximation

Table 1 Effects of the micelle composition (α_M) on the aggregation number of micelles (m), the apparent electrical charge (ze_0), the degree of counterion binding (θ), the effective surface potential (ψ_0) and the semiaxes (a, b) of the ellipsoid of rotation

α_M	m	z	θ	ψ_0/mV	b/A	a/A	$\langle d \rangle$/A
0	78 ± 2	0	0	0	20 ± 2	46 ± 3	
0.29 ± 0.01	77 ± 2	10 ± 1	0.55 ± 0.02	50 ± 2	21 ± 2	38 ± 2	105 ± 5
0.37 ± 0.01	74 ± 2	14 ± 1	0.49 ± 0.02	64 ± 2	21 ± 2	37 ± 2	118 ± 8
0.52 ± 0.01	70 ± 2	17 ± 2	0.53 ± 0.02	70 ± 3	21 ± 2	35 ± 2	115 ± 8
0.73 ± 0.01	73 ± 2	17 ± 2	0.68 ± 0.03	68 ± 3	21 ± 2	36 ± 2	113 ± 8

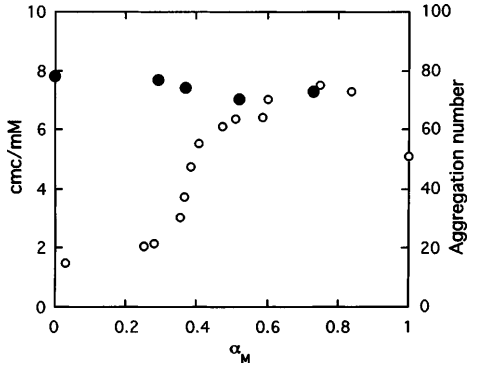

Fig. 2 Dependence of the aggregation number, m, from small-angle neutron scattering (*SANS*) and the critical micelle concentration (*cmc*) on the micelle composition, α_M. (○): The cmc values taken from Ref. [15]; (●): the aggregation number

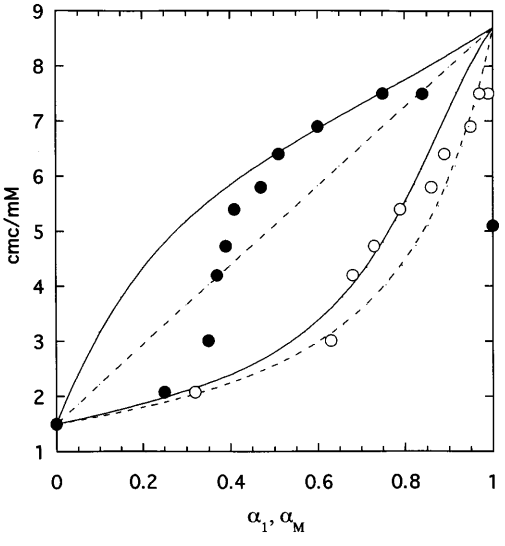

Fig. 3 Composition dependence of the cmc compared with the regular solution model. Experimental cmc values are plotted against the micelle composition, α_M, (●) and the monomer composition, α_1, (○). Calculated dependence from the regular solution model: *solid* and *broken curves* refer to the cases of $\beta = 0.9$ and $\beta = 0$, respectively

with more negative interaction parameter values, β, than those at moderate-to-high ionic strengths [33]. It is to be noted, however, that in most previous studies only the dependence on the monomer composition, α_1, has been examined. Also in the present case, the plot (cmc versus α_1) does not show a marked deviation and the data could be fitted with $\beta = 0$–0.9. The failure of the regular solution approximation becomes evident only when the dependence on the micelle composition is examined. It should be stressed that amine oxides are rare surfactants in the sense that both compositions, α_M and α_1, can be determined experimentally by hydrogen ion titration. In contrast with this rather unusual cmc behaviour, the size of the micelle scarcely changes with α_M. The aggregation numbers of about 78 in Fig. 2 are comparable with that of 70 for nonionic micelles in solutions with no added salt [1] and with those in 0.1 M and 0.2 M NaCl solutions: about 70 from static light scattering and 90 and 80 from the fluorescence probe method [11].

The degree of counterion binding, θ, related to z as $\theta = 1 - z/(m\,\alpha_M)$. The results were in fair agreement with those from the counterion activity: 0.72, 0.62, 0.52, 0.55, 0.32, 0.52, 0.23 for α_M of 0.79, 0.69, 0.47, 0.43, 0.34, 0.26 and 0.19, respectively [15]. This counterion binding is taken into account in the evaluation of the surface potentials, ψ_0, appearing in Eqs. (7) and (8). Values of ψ_0 were 50–70 mV and are given in Table 1 together with θ values.

Effects of salt concentration on the scattering curves

The addition of salt gives rise to scattering in both cases of the cationic (Fig. 4A) and the 1:1 composition (Fig. 4B) but the effect is more significant for the cationic species. We did not observe interference in the scattering curves and one can assume that the salt screens the electrical interaction completely. At a salt concentration, c_s, of 3 M, phase separation took place for both solutions. The shapes of the scattering curves are similar for both the cationic and the 1:1 composition with salt addition. In a low q region one can observe the cylindrical signature

$$d\Sigma(q)/d\Omega \sim q^{-1} \exp(-R_c^2 q^2/4) \quad , \tag{9}$$

where R_c is the radius of gyration of the cross section of the cylinder. This analysis gave a value of R_c approximately equal to 12 Å or R in the homogenous approximation is equal to 17 Å. The experimental curves are analyzed in terms of the assumed cylindrical micelles in

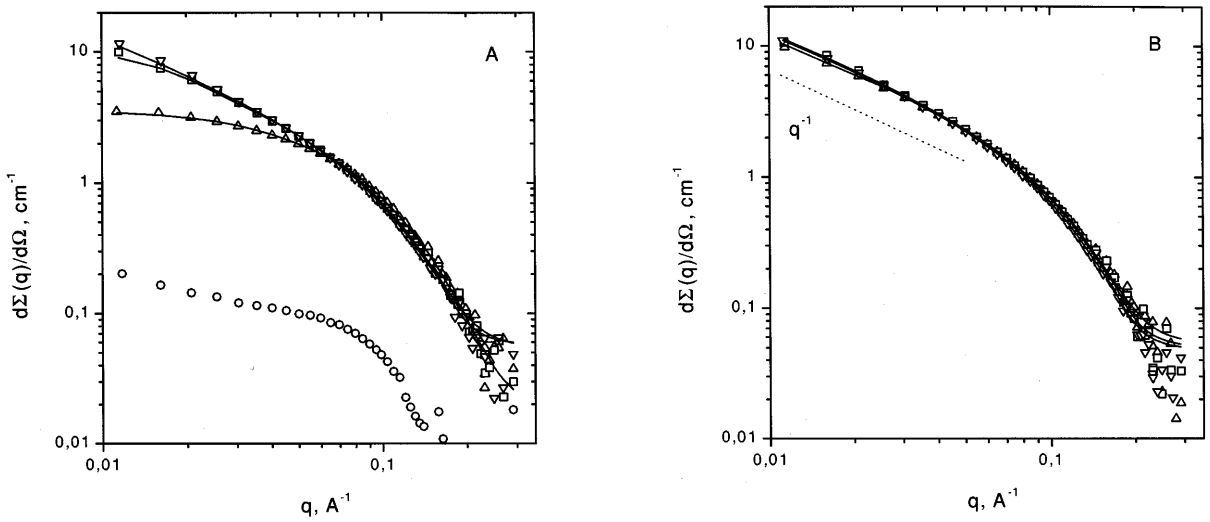

Fig. 4A, B Effects of NaCl concentration, c_s, on the SANS of DDAO solutions. Surfactant concentration c_D = 50–55 mM. NaCl concentration c_s/M: 0.22 (▽), 0.55 (□), 1.1 (Δ) and 3 (○). Micelle compositions: **A** cationic micelle (α_M = 1) and **B** 1:1 composition (α_M = 0.5). *Solid curves* represent the fitting curves

the solution. In this case we used the form factor for a cylinder, Eq. (10), as the F function in Eq. (5) to model the scattering from separate particles.

$$F(q,R_i) = \frac{\sin(qL/2\cos\beta)2J_1(qR_i\sin\beta)}{(qL/2\cos\beta)(qR_i\sin\beta)} \quad , \qquad (10)$$

where L is the length of the cylinder, $R_1 = R_{in}$ and $R_2 = R_{out}$ are the inner and outer radii of the cylinder, J_1 is the first-order Bessel function and β is the angle between the q vector and the axis of the cylinder. The volumes of the inner and the outer parts of cylinder were calculated using Eq. (6) with assumption that $\theta = 1$.

To model the interaction among aggregates we used the structure factor of a hard-sphere fluid calculated in the Percus–Yevick closure of the correlation function [34]. In this case, $S(q)$ can be written as

$$S(q) = [1 + 24\eta G(y)/y]^{-1} \quad , \qquad (11)$$

with $y = 2qR_{hs}$. R_{hs} is the radius of the hard-sphere interaction which is calculated by $R_{hs} = (0.75\,R_{out}^2 L)^{1/3}$. η is the volume fraction of hard spheres. The function $G(y)$ is given explicitly in Ref. [35]. The differential cross section of neutron scattering $d\Sigma(q)/d\Omega$ is calculated in the decoupling approximation Eq. (4).

The fitting parameters are the aggregation number, the volume of the hard-sphere interaction, the hydration number, the residual background and the normalization parameter. The radius of inner part was fixed at 11.6 Å. The parameters obtained are presented in Table 2.

As shown in Table 2, the micelles of both the cationic and the 1:1 composition grow with NaCl concentration between 0.22 and 0.55 M, while very little change is seen between 0.55 and 1.09 M. The size of the micelles of 1:1 composition is greater than that of the cationic composition, and this is consistent with previous findings [11]; at a high c_s of 1 M they become similar. The present results clearly indicate that the previously suggested micelle growth takes place by the transformation into rodlike micelles.

ELS from solutions with no added salt

To examine further the properties of the solutions with no added salt, we performed ELS measurements. The

Table 2 Dependence on NaCl concentration (c_s) of the aggregation number of micelles (m), the hydration number (N_{hyd}), the length (L) and outer radius (R_{out}) of a model cylinder, and the volume of the hard-sphere interaction (η)

Micelle composition	α_M	c_s/M	m	N_{hyd}	L/A	R_{out}/A	$\eta/10^{-2}$
1:1	0.50	0.22	670 ± 30	5.0 ± 1.0	560 ± 20	22.2 ± 1.2	2.0 ± 0.3
1:1	0.50	0.55	900 ± 40	5.3 ± 1.0	750 ± 20	23.2 ± 1.2	[a]
1:1	0.50	1.1	910 ± 40	5.6 ± 1.0	760 ± 20	23.7 ± 1.3	[a]
Cationic	1.0	0.22	160 ± 10	3.0 ± 0.5	130 ± 7	20.0 ± 1.0	6.2 ± 0.5
Cationic	1.0	0.55	820 ± 30	5.0 ± 1.0	670 ± 20	22.0 ± 1.0	5.0 ± 0.5
Cationic	1.0	1.1	920 ± 40	5.5 ± 1.0	760 ± 20	23.5 ± 1.2	[a]

[a] Below the detection limit

Table 3 Summary of the electrophoretic light scattering on the solutions with no added salt. Dodecyldimethylamine oxide concentration: 30 mM

α_M	$u/10^{-4}$ cm^2 V^{-1} s^{-1}	Zeta potential/mV	$D_{app}/10^{-6}$ cm^2 s^{-1}	$R_{H,app}$/nm
0.20 ± 0.1	1.8 ± 0.1	35 ± 2	0.69 ± 0.02	3.6 ± 0.2
0.39 ± 0.1	2.1 ± 0.1	41 ± 2	1.89 ± 0.05	1.3 ± 0.1
0.60 ± 0.1	3.3 ± 0.1	63 ± 3	1.10 ± 0.03	2.2 ± 0.2
0.76 ± 0.1	5.0 ± 0.2	96 ± 5	1.53 ± 0.05	1.6 ± 0.1
0.81 ± 0.1	4.2 ± 0.1	81 ± 5	1.62 ± 0.05	1.5 ± 0.1

values of the electrophoretic mobility, u, and the zeta potential, ζ, are given in Table 3. From SANS measurement (Table 1), a rough estimate of the radius, a, of the equivalent sphere is in the range 2.5–3 nm. As shown in Fig. 2, on the other hand, the cmc varies between 2 and 7 mM and hence κa is about unity or less for the present measurements. This means the Henry function takes values close to unity and therefore we used the Hückel equation rather than the Smoluchowski equation to evaluate the zeta potentials. The values obtained could be taken as the upper bound. The zeta potentials were in the range 35–96 mV. It is to be noted that the relaxation effect is ignored in the present evaluation. It is also to be noted that the applied electric field may alter the pH of the solutions and hence α_M. To examine the properties with no added salt, however, we did not employ any buffer to avoid an increase in the ionic strength.

From the dynamic light scattering (DCS) measurements, we obtained the hydrodynamic radius of the equivalent sphere (R_H) as shown in Table 3. The R_H values remain essentially constant (1.8 ± 0.5 nm) independent of α_M. This relative independence of α_M is consistent with the SANS results. Aside from the composition dependence, the magnitude of R_H (1.8 ± 0.5 nm) will be discussed here. Since the DLS measurements were made in media of rather low ionic strength, there remains the question of whether the observed diffusion constant, D_{app}, can be approximated by the self-diffusion constant of the micelles, D_m. For macroion solutions of low ionic strength, considerable coupling of motion is expected between macroions and small ions. On the other hand, we also measured D_{app} for the nonionic species ($\alpha_M = 0$) and R_H was about 1.5 nm which is rather similar to R_H values in Table 3. This result suggests that the coupling between micelle ions and Cl counterions is not significant and that the R_H values given in Table 3 are not far from the correct values.

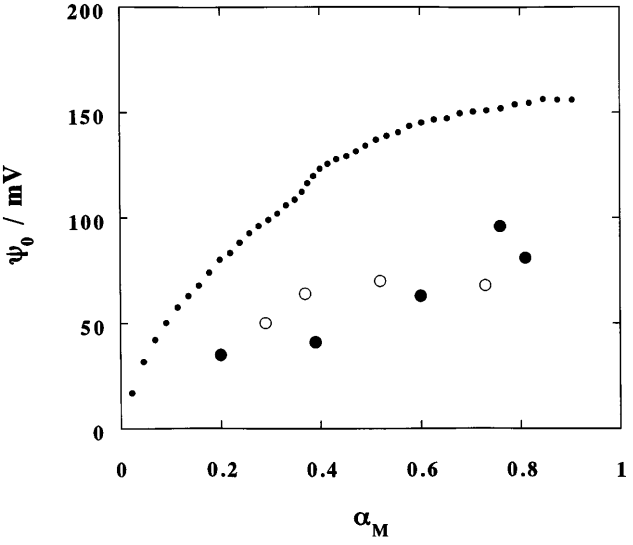

Fig. 5 Comparison of three surface potentials of the micelles at different micelle compositions, α_M. (•) The actual surface potentials determined from hydrogen ion titration [15]. (○) The effective surface potentials from SANS. (●) The zeta potentials from electrophoretic light scattering

Discussion

Intermicelle interactions

As shown in Table 1, the SANS measurements gave the effective surface potential, ψ_0, responsible for the intermicelle interaction in the solutions with no added salt. On the other hand, we have determined the actual surface potentials, ψ_0^H, by hydrogen ion titration [15]. ψ_0 and ψ_0^H are compared in Fig. 5 and ψ_0 is seen to be much smaller that ψ_0^H. We cannot use the linearization approximation, Eqs. (7) and (8), if we put $\psi_0 = \psi_0^H$, however, the mutual electric repulsion between the micelles is so great that we can approximate the interaction with the equivalent hard sphere carrying the effective number of charges, instead of elaborating the intermicelle electric interaction without the linear approximation. The diameter $\langle d \rangle$ in Eqs. (7) and (8) should be much larger than what is expected from the actual prolate particles characterized with the semiaxes a and b given in Table 1. To compare $\langle d \rangle$ with the distance at the slipping plane, it is interesting to compare ψ_0 with the zeta potential from ELS as shown in Fig. 5, they are in fair agreement with each other. We thus find that the potential operating in the electric repulsion between the micelles is rather close to the zeta potential. The agreement suggests the dimension of the effective hard sphere is close to the distance between the slipping plane and the centre of the micelle.

The smaller dimension of the aggregates and the molecular structure

In the present study, we employed two shell prolates and two shell cylinders for the micelles. The smaller dimension of these models, either b or R_{out}, is expected to be closely related to the molecular structure of amine oxide.

According to Tanford [27], the length of the hydrocarbon chain l_c for a dodecyl group is in the range 1.54 (fully extended)–1.16 nm (flexible). The length of the surfactant molecule with a desolvated head group is $l_c + 0.49$ nm in the present case. Since the radius of hydrated chloride counterions is 0.33 nm, we can expect b or R_{out} to range from $l_c + 0.49$ (without counterion binding) to $l_c + 1.15$ nm (with a bound counterion). It is to be noted that the hydration of the polar head group is not taken into account in these estimates. From Table 1, values of b are in the range 2.0–2.1 nm. This suggests that l_c is close to 1.16 nm and the hydrocarbon chains are flexible, which is consistent with the generally accepted picture of the liquidlike nature of the interior of the micelles. So, in the analyses of the salt effect, we set l_c to 1.16 nm. The results for R_{out} given in Table 2 fall in the range 2.0–2.4 nm. These values are quite reasonable in light of the previous discussion. SANS studies on surfactants sometimes report aggregate sizes inconsistent with the molecular parameters given here. This may reflect the roughness of micelle surfaces. However, in the present study we obtained dimensions consistent with the molecular structure.

Acknowledgements We thank Dr. T. Takagi, Institute for Protein Research, Osaka University, for kindly giving us the facilities concerning the ELS measurements and Yukiko Imaishi for her help with the ELS measurements.

References

1. Herrmann KW (1962) J Phys Chem 66:295–300
2. Benjamin L (1964) J Phys Chem 68:3575–3581
3. Tokiwa F, Ohki K (1966) J Phys Chem 70:3437–3441
4. Maeda H, Tsunoda M, Ikeda S (1974) J Phys Chem 78:1086–1090
5. Funasaki N (1977) J Colloid Interface Sci 60:54–59
6. Hoffmann H, Oetter G, Schwandner B (1987) Prog Colloid Polymer Sci 73:95–106
7. Rathman JF, Christian SD (1990) Langmuir 6:391–395
8. Rathman JF, Scheuing DR (1990) ACS Symp Ser 447:123–142
9. Zhang H, Dubin PL, Kaplan JI (1991) Langmuir 7:2103–2107
10. Brackman JC, Engberts JBFN (1992) Langmuir 8:424–428
11. Kaimoto H, Shoho K, Sasaki S, Maeda H (1994) J Phys Chem 98:10243–10248
12. Maeda H, Muroi S, Ishii M, Kakehashi R, Kaimoto H, Nakahara T, Motomoura K (1995) J Colloid Interface Sci 175:497–505
13. Maeda H (1996) Colloids Surf A 109:263–271
14. Maeda H, Muroi S, Kakehashi R (1997) J Phys Chem B 101:7378–7382
15. Imaishi Y, Kakehashi R, Nezu T, Maeda H (1998) J Colloid Interface Sci 197:309–316
16. Alargova RG, Vakarelsky IY, Paunov VN, Stoyanov SD, Kralchevsky PA, Mehreteab A, Broze G (1998) Langmuir 14:1996–2003
17. Hoffmann H (1990) Prog Colloid Polym Sci 83:16–28
18. Chen H (1986) Annu Rev Phys Chem 37:351–399
19. Chen SH, Huang JS, Tartaglia P (1992) Structure and dynamics of strongly interacting colloids and supramolecular aggregates in solution. Kluwer Dordrecht
20. Garamus VM (1997) Langmuir 13:6388–6392
21. Gorski N, Gradzielski M, Hoffmann H (1994) Langmuir 10:2594–2603
22. Gorski N, Kalus J (1997) J Phys Chem B101:4390–4393
23. Ostanevich Yu M (1988) Makromol Chem Macromol Symp 15:91–96
24. Kozlova EP, Ostanevich Yu M, Cser L (1980) Nucl Instrum Methods 169:597–605
25. Glatter O, Kratky O (1982) Small-angle X-ray scattering. Academic Press, London
26. Kotlarchyk M, Chen SH (1983) J Chem Phys 79:2461–2469
27. Tanford C (1980) The hydrophobic effect, 2nd edn. J Wiley, New York, pp 51–53
28. Berr SS, Jones RRM, Johnson JS (1992) J Phys Chem 96:5611–5614
29. Verwey EJW, Overbeek J Th G (1948) Theory of the stability of lyophobic colloids. Elsevier, New York, Chapter X
30. Hansen JP, Hayter JB (1982) Mol Phys 46:651–656
31. Taupin D, Luzzati V (1982) J Appl Crystallogr 15:289–300
32. Rubingh DN (1979) In: Mittal K (ed) Solution chemistry of surfactants. Plenum, New York, pp 337–354
33. Holland PM (1986) Adv Colloid Interface Sci 26:111–129
34. Wertheim MS (1963) Phys Rev Lett 10:312–320
35. Kinning D, Thomas E (1984) Macromolecules 17:1712–1721